THE THERMAL STABILITY OF NANOSTRUCTURED FERRITIC ALLOYS—P. Miao, G. R. Odette, T. Yamamoto, and D. Klingensmith (University of California, Santa Barbara)

OBJECTIVE

The objective of this work was to characterize the stability of the microstructure and mechanical properties for a nanostructured ferrite alloy, MA957, under high temperature thermal aging conditions.

SUMMARY

The excellent tensile and creep strength and the potential for managing radiation damage make nanostructured ferritic alloys (NFAs) promising candidates for high temperature applications in spallation proton, advanced fission, and fusion neutron environments. The thermal stability of NFAs is critical for such applications, hence, this has been investigated in a series of aging experiments on MA957 at 900˚C, 950˚C, and 1000˚C for times up to 8000 h. Optical and transmission electron microscopy (TEM) studies for 3000 h aged MA957 showed the fine scale grain and dislocation structures are stable up to 1000°C. TEM and small angle neutron scattering (SANS) showed that the nm-scale solute cluster-oxide features (NFs), that are a primary source of the high strength of NFAs, were stable at 900°C and coarsened only slightly at 950˚C and 1000˚C after 3000 h aging. Porosity that developed during high temperature aging was minimal at 900°C and modest at 950˚C, but was much larger after 1000°C. Microhardness for the 3000 h aged MA957 was basically unchanged after the 900°C aging and decreased only slightly (≤ 3%) after aging at 950˚C and 1000˚C. However, the hardness was significantly reduced after 8000 h aging at 1000˚C.

PROGRESS AND STATUS

Introduction

Nanostructured ferritic alloys (NFAs) have outstanding low-temperature tensile and high-temperature creep strength [1 - 9] and the potential for managing radiation damage [1, 10, 11], including high helium levels in fusion, advanced fission, and spallation proton environments. The excellent properties of NFAs primarily derive from a high density of nm-sized Y-Ti-O precipitate cluster and/or complex oxides, such as $Y_2Ti_2O_7$ and Y_2TiO_5, which form during hot consolidation following mechanical alloying [1, 7, 12-18]. The nm-scale features (NFs) are reported to be stable, at least for a limited range of irradiation conditions [1, 10, 19-21]. A key issue for NFAs is stability of their excellent properties and microstructures at high temperatures.

The high temperature and short time thermal stability of NFAs were previously investigated in a series of aging experiments of MA957 at 1150 to 1400˚C for various times ranging from 1/3 to 480 h. These experiments showed significant coarsening of the NFs, rapid growth of porosity, and large decrease of microhardness with increasing aging temperature and time [7, 12]. However, the aging temperatures in these experiments were much higher than those that are expected for application of NFAs, in the range from ≈ 650 to 850°C. Indeed, fits of kinetic coarsening models yielded parameters for the high temperature aging data that predict very high NF stability at lower temperatures. Analysis of the aging data covering the initial period of coarsening, at NF sizes less than 5-6 nm, yielded activation energies in excess of 850kJ/mole and a $t^{1/5}$ time-dependence [7, 12]. Atom probe tomography studies have also suggested that the NFs are remarkably stable at high temperature and during creep [17, 22]. Thus, to confirm these observations, we initiated a series of aging experiments of MA957 at temperatures from 800 to 1000˚C for planned times up to 20,000 h or more. Interim microstructure, NF analysis, and hardness results on the effects of aging at 900˚C, 950˚C, and 1000˚C up to 3000 h and the hardness results for 8000 h aging at 900˚C and 1000˚C are reported here.

Experimental Procedure

Coupon specimens of as-received MA957 alloy extruded at 1150°C with a nominal composition of Fe-14wt% Cr, 0.9% Ti, 0.3% Mo, and 0.25% Y_2O_3 were thermally aged for 3000 h at 900˚C, 950˚C, and 1000˚C and for 8000 h at 900˚C and 1000˚C in quartz capsules which were vacuum evaporated and backfilled with dry helium at 50kPa.

The coarser scale and NF microstructures of the as-extruded and the 3000 h aged MA957 were characterized using optical microscopy, TEM (JEOL2010HR), and SANS (NG7 at the National Institute of Standards and Technology). Standard 3 mm TEM discs, taken from a region of ≈ 1mm away from sample surface, were ground to a thickness of ≈ 0.15 mm and then thinned to electron transparency in a TENUPOL twin-jet electro-polisher with H_2SO_4 + 80%CH_3OH at room temperature. The thinned samples were carefully washed in methanol, transformed to a vacuum desiccator, and then loaded to TEM for observation within one hour to minimize contamination. TEM images for the measurement of the NFs were taken in a near the [011] orientation. The thickness of the TEM samples was measured by the convergent beam diffraction technique. Details of the experiment, data reduction, and analysis for SANS are given elsewhere [7].

Mechanical properties of the MA957 samples were evaluated by Vickers microhardness at a 500g load.

Results

As shown in the TEM micrographs in Figs. 1 and 2 in a region ≈ 1mm away below the sample surface, the as-extruded MA957 has fine ferrite grains and a high dislocation density (Figs. 1a and 2a) that remain stable after 3000 h aging at 900°C, 950°C, and 1000°C (Figs. 1b and 2b, 1c and 2c, 1d and 2d). Note that ferrite grains in a very thin layer (≤ 30μm for 950°C and ≤ 200μm for 1000°C) close to the sample surfaces coarsened at 950°C and 1000°C. Composition analysis of these regions indicates that the local coarsening was due to the sublimation of the elements like Cr. Thus protection coatings, like alumina scale, will be needed to use NFAs at temperatures higher than 900°C in environments such as helium coolants.

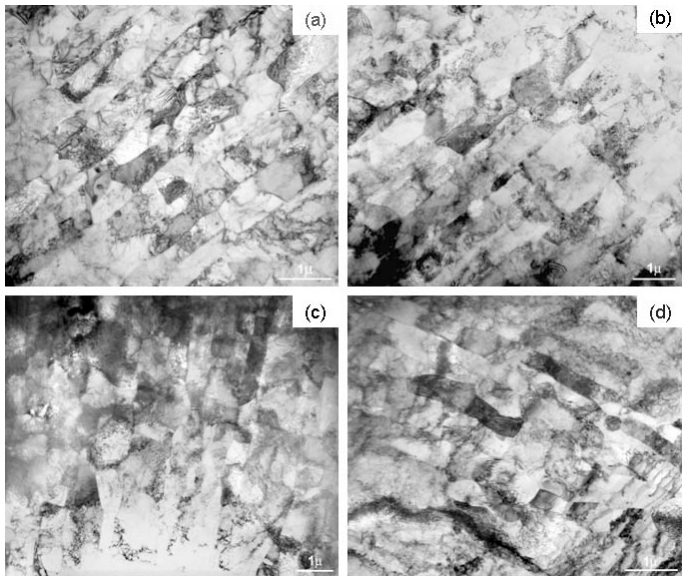

Fig. 1. TEM micrographs of (a) the as-extruded MA957 and MA957 aged for 3000 h at (b) 900°C, (c) 950°C, and (d) 1000°C.

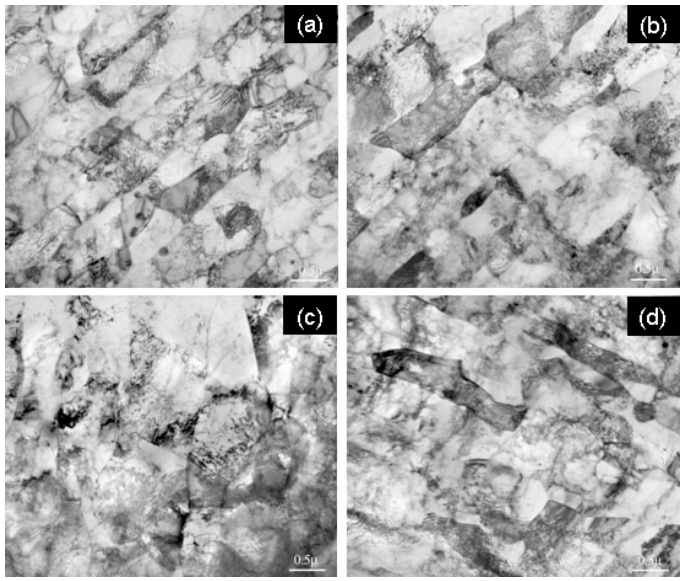

Fig. 2. Higher magnification of Fig. 1, showing dislocations in (a) the as-extruded MA957 and MA957 aged for 3000 h at (b) 900°C, (c) 950°C, and (d) 1000°C.

The as-extruded and the aged MA957 contain a large number of NFs, as seen in Fig. 3. Their diameter (d), number density (N), and volume fraction (f) were measured using computer assisted image analysis of TEM micrographs and convergent beam estimates of the foil thickness. These data are shown in Figs. 4 and 5. Large particles, with diameters greater than ≈ 10 nm, were not included in the measurements. The average diameters are 2.1±0.4, 2.1±0.4, 2.6±0.5, and 3.1±0.9 nm for the as-extruded and the 900˚C/3000h, 950˚C/3000h, and 1000˚C/3000h aged MA957, respectively. The corresponding total number density of NF after 900˚C aging is similar to that for the as-extruded MA957, within the uncertainties associated with single area measurements, resolution limits, and other possible sources of error. However, the number densities of NF decrease significantly after 950˚C and 1000˚C aging. Nevertheless, the total volume fraction did not change significantly. Note these evaluations are in qualitative agreement with measurements by SANS. The absence of coarsening at 900˚C, which does occur at 950˚C and 1000˚C, is more clearly shown in the number density distribution histograms presented in Fig. 5. The NF distributions at 900˚C are nearly the same as those in the as-extruded, but they shift to larger diameters at 950˚C and even more so at 1000˚C.

The NF coarsening at 1000°C was also qualitatively confirmed by the SANS experiment, as shown in Fig. 6. The open and filled symbols are the NF scattering cross sections measured at 45° to the magnetic field (this includes the nuclear plus 50% of the magnetic scattering) as a function of the square of the scattering vector, q, for the as-extruded and 1000°C-3000 h aged conditions, respectively. The decrease in the magnitude of $d\Sigma/d\Omega$ versus q^2 for 1000°C-aged MA957 at higher q and increase at very low q in the aged condition indicates a slight coarsening of the NFs.

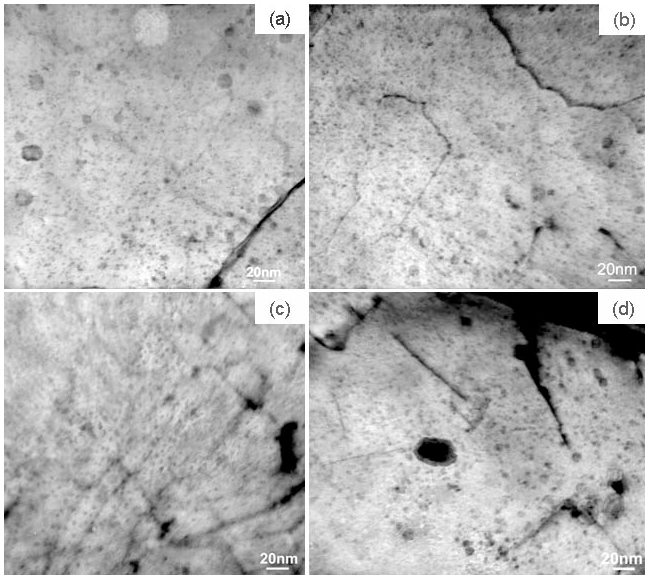

Fig. 3. NFs in (a) the as-extruded MA957 and MA957 aged for 3000 h at (b) 900°C, (c) 950°C, and (d) 1000°C.

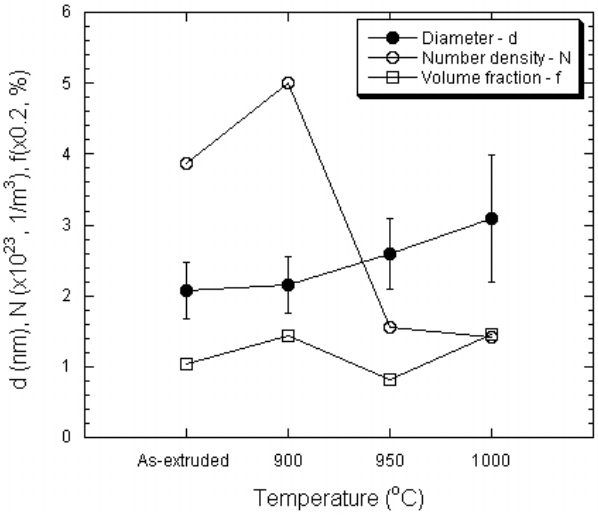

Fig. 4. Average diameter, total number density, and volume fraction of NFs in the as-extruded and aged MA957.

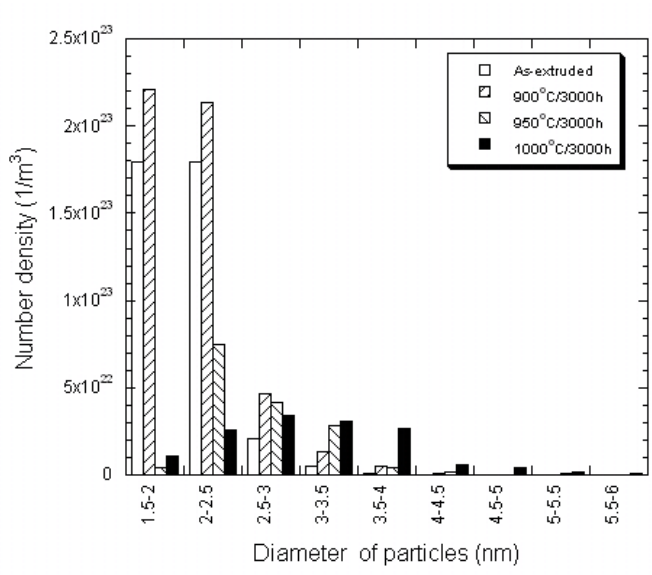

Fig. 5. Number density distribution of NFs in the as-extruded and aged MA957.

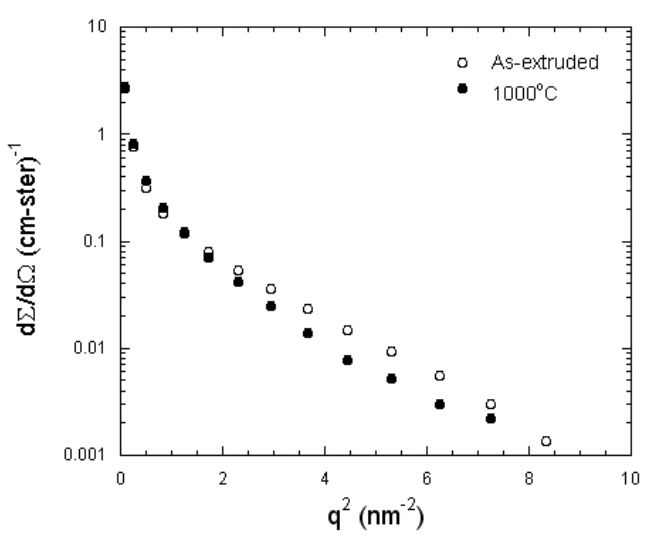

Fig. 6. SANS cross section curves at a 45° angle to the direction of the magnetic field.

Porosities of the as-extruded and the 3000 h aged MA957 were measured on optical micrographs of as-polished cross-sections normal to the extrusion are shown in Table 1 and illustrated in Fig. 7. The pore diameters and area fractions increased ≈ 25% and 200%, respectively, after aging at 900°C and 950°C, respectively. Much of this increase is due to the growth of pores that are visible in the as-received condition; however, as indicated in Table 1, the pore density may also increase slightly due to the growth of previously invisible submicron-sized pores [23] formed during mechanical alloying. The average diameter and area fraction of the pores grow much more significantly after aging at 1000°C, with increases of ≈ 350% and 1150%, respectively. The apparent decrease in the number density of pores may be due to coalescence.

Table 1. Average diameter, area fraction, and number density of pores

Heat treatment	Average diameter of pores (μm)	Area fraction of pores (%)	Number density of pores ($\times 10^9$, $1/m^2$)
As-extruded	2.2±1.2	0.5	1.0
900°C/3000h	2.8±2.4	1.5	1.4
950°C/3000h	2.7±2.5	1.2	1.1
1000°C/3000h	10.1±8.7	6.2	0.5

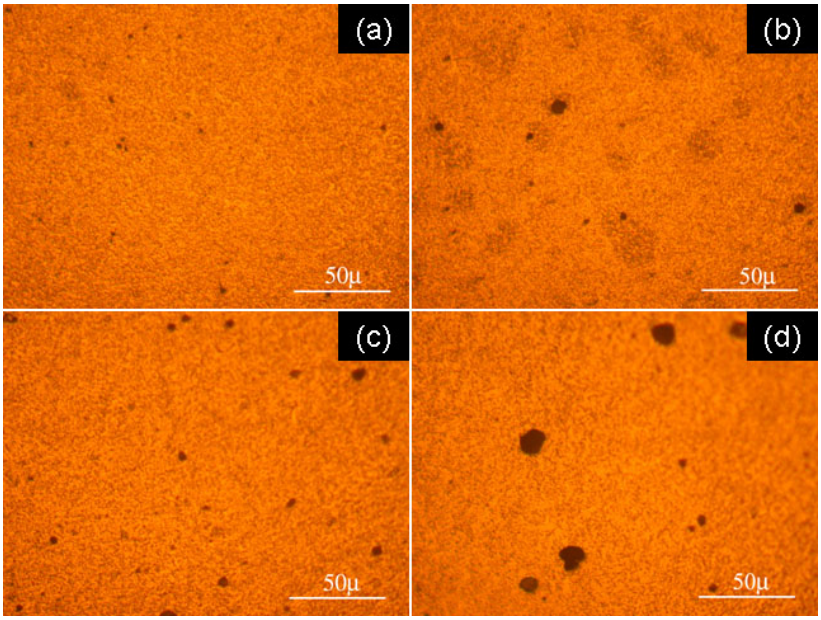

Fig. 7. Optical micrographs in cross-sections normal to the extrusion direction of (a) the as-extruded MA957 and MA957 aged for 3000 h at (b) 900°C, (c) 950°C, and (d) 1000°C. Note that the black features in (a) – (d) are pores.

Vicker's diamond pyramid hardness (DPH, kg/mm^2) measurements on polished cross-sections parallel to the extrusion direction are shown in Table 2. The measurements were made at ≈ 1mm (for 3000 h aging) and ≈ 1.5mm (for 8000 h aging) depth, which is sufficient to avoid the artifacts associated with the near surface environmentally induced instabilities noted above. Slight softening is observed after 3000 h aging but is insignificant (< 1%) except perhaps at 950°C, where the DPH decreases by ≈ 3%. However, given the one standard deviation uncertainties in the hardness of ≈ ± 6 to 8 DPH, it is concluded that softening after 3000 h aging is minimal to non-existent.

The microhardness of MA957 aged for 8000 h at 900°C is nearly the same as those for the 3000 h aged MA957, but it is significantly reduced after 8000 h aging at 1000°C.

Table 2. DPH of as-extruded and aged MA957

Heat treatment	As-extruded	900°C		950°C	1000°C	
		3000 h	8000 h	3000 h	3000 h	8000 h
DPH	333±8	332±7	325±8	323±7	330±6	306±6

Discussion

The SANS investigation [7] of MA957 after high temperature (1150°C - 1250°C) and short-time (1/3 – 480 h) aging showed significant NF coarsening. The data in the initial coarsening regime for aging at 1150°C to 1250°C for 1/3 to 480 h were least square fitted using expression with the form

$$d(T,t) = d_0[tk'_{co}\exp(-Q_{ec}/RT)+1]^p \qquad (1)$$

Here d_0 and d(T, t) are the NF sizes before and after aging, respectively, t is the aging time, T is the aging temperature (°K), and R is the gas constant. The fits yielded a rate coefficient, k'_{co} = 2.94×10^{27}/s, an effective activation energy for coarsening, Q_{ec} ≈ 884kJ/mole, and a time scaling exponent, p = 0.2. The fitted p is consistent with a dislocation pipe diffusion mechanism, but the rather remarkably high value of Q_{ec} is not well understood. Assuming a d_0 = 2.6 nm for the as-extruded MA957 based on SANS measurement [7], predictions of Equation 1 for high temperature aging for 3000 h are shown by the open circles in Fig. 8, along with the longest time data from the previous high temperature aging study. Extrapolations of Equation 1 to lower temperatures predict insignificant coarsening below ≈ 1050 °C. Thus, the high temperature aging model is somewhat inconsistent with the current lower temperature results at 950°C and 1000°C. While the coarsening is modest even at 1000°C and does not lead to significant softening, data at longer times will be needed to refine the aging model for predicting thermal stability in the application regime for NFAs below ≈ 850°C.

The small hardness changes at 1000°C and 3000 h in spite of the NF coarsening is consistent with previous estimates of the relation between the strengthening contribution of the NFs and their corresponding d and f [7]. This work showed that the individual NF contribution to the yield stress is proportional to HP = log(d/4b)b/d, where HP is a hardening parameter and b is the Burgers vector (0.25 nm) for Fe. Figure 9 shows that the HP plotted versus d has a broad maximum, peaking around d ≈ 2.5 nm; the predicted HP actually increases slightly between d = 2 and 2.5 nm and is almost constant between d = 2.5 and 3 nm.

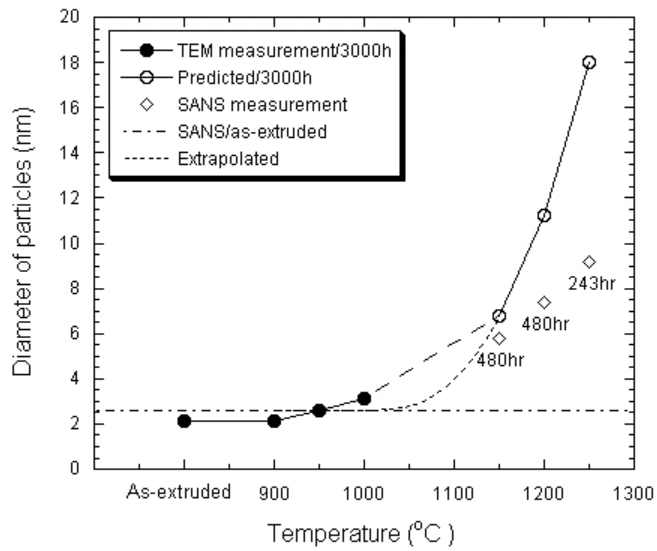

Fig. 8. Size variation of NFs with temperature for the as-extruded and the aged MA957. The filled circles: NF sizes measured by TEM, the open diamonds: NF sizes measured by SANS, and the open circles: NF sizes predicted using equation 1 for 1150°C/3000h, 1200°C/3000h, and 1250°C/3000h aging.

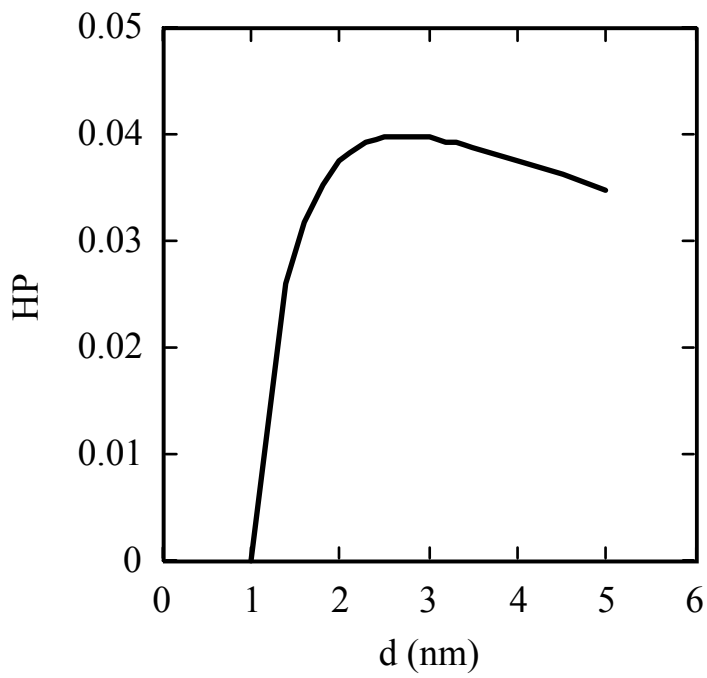

Fig. 9. Variation of hardening parameter (HP) with the NF size (d).

SUMMARY AND CONCLUSIONS

The interim MA957 aging data show that the fine ferrite grains and high dislocation densities are thermally stable at 900˚C, 950˚C, and 1000˚C for 3000 h. The NFs are thermally stable at 900˚C, but coarsen slightly at 950˚C and 1000˚C for 3000 h aging. However, the NF coarsening did not lead to significant softening, consistent with expectation. The growth porosity is much smaller at 900˚C and 950˚C compared with the 1000˚C aging.

Future Work

The aging experiments are continuing at all temperatures. Emphasis during the next reporting period will be on detailed microstructural characterization of the specimens aged for 8000 h and additional hardness measurements for the longest aging times at all temperatures.

References

[1] M. L. Hamilton, D. S. Gelles, R. J. Lobsinger, G. D. Johnson, W. F. Brown, M. M. Paxton, R. J. Puigh, C. R. Eiholzer, and M. A. Blotter, Fabrication technological development of the oxide dispersion strengthened alloy MA957 for fast reactor applications, PNNL-13168 (released 2000), (1991).
[2] C. Zakine, C. Prioul, and D. Francois, Mater. Sci. Eng., A 219 (1996) 102.
[3] S. Ukai, T. Okuda, M. Fujiwara, T. Kobayashi, S. Mizuta, and H. Nakashima, J. Nucl. Sci. Technol. 39(8) (2002) 872.
[4] S. Ukai and M. Fujiwara, J. Nucl. Mater. 307-311 (2002) 749.
[5] M. J. Alinger, G. R. Odette, and G. E. Lucas, J. Nucl. Mater. 307-311 (2002) 484.
[6] R. L. Klueh, P. J. Maziasz, I. S. Kim, L. Heatherly, D. T. Hoelzer, N. Hashimoto, E. A. Kenik, and K. Miyahara, J. Nucl. Mater. 307-311 (2002) 773.
[7] M.J. Alinger, On the formation and stability of nanometer scale precipitates in ferritic alloys during processing and high temperature service, Ph.D. thesis, University of California, Santa Barbara (2004).
[8] A. Alamo, V. Lambard, X. Averty, and M. H. Mathon, J. Nucl. Mater. 329–333 (2004) 333.
[9] B. Wilshire and T. D. Lieu, Mater. Sci. Eng., A 386 (2004) 81.
[10] T. Yamamoto, G. R. Odette, P. Miao, D. T. Hoelzer, J. Bentley, N. Hashimoto, H. Tanigawa, and R. J. Kurtz, Journal of Nuclear Materials (2007) doi:10.1016/j.jnucmat.2007.03.047.
[11] D. S. Gelles, J. Nucl. Mater. 233-237 (1996) 293.
[12] M. J. Alinger, G. R. Odette, and D. T. Hoelzer, J. Nucl. Mater. 329-333 (2004) 382.
[13] S. Yamashita, S. Ohtsuka, N. Akasaka, S. Ukai, and S. Ohnukiy, Philos. Mag. Lett. 84(8) (2004) 525.
[14] M. Klimiankou, R. Lindau, and A. Moslang, J. Nucl. Mater. 329-333 (2004) 347.
[15] H. Kishimoto, M. J. Alinger, G. R. Odette, and T. Yamamoto, J. Nucl. Mater. 329-33 (2004) 369.
[16] M. Klimiankou, R. Lindau, and A. Moslang, Micron 36 (2005) 1.
[17] M. K. Miller, D. T. Hoelzer, E. A. Kenik, and K. F. Russell, Intermetallics 133-134 (2005) 387.
[18] M. K. Miller, K. F. Russell, and D. T. Hoelzer, J. Nucl. Mater. 351 (2006) 261.
[19] S. Yamashita, K. Oka, S. Ohnuki, N. Akasaka, and S. Ukai, J. Nucl. Mater. 307-311 (2002) 283.
[20] S. Yamashita, N. Akasaka, and S. Ohnuki, J. Nucl. Mater. 329-333 (2004) 377.
[21] P. Pareige, M. K. Miller, R. E. Stoller, D. T. Hoelzer, E. Cadel, and B. Radiquet, J. Nucl. Mater. 360 (2007) 136.
[22] M. K. Miller, D. T. Hoelzer, E. A. Kenik, and K. F. Russell, Microsc. Microanal. 10 (Suppl. 2) (2004) 708.
[23] Y. L. Chen, A. R. Jones, and U. Miller, Metall. Mater. Trans. A 33A (2002) 2713.